Curr Cardiovasc Imaging Rep (2014) 7:9290
DOI 10.1007/s12410-014-9290-0

INTRAVASCULAR IMAGING (E REGAR AND U LANDMESSER, SECTION EDITORS)

Development of 3D IVOCT Imaging and Co-Registration of IVOCT and Angiography in the Catheterization Laboratory

Dries De Cock · Shengxian Tu · Giovanni J. Ughi · Tom Adriaenssens

Published online: 13 August 2014

Abstract Intravascular optical coherence tomography (IVOCT) has become the imaging modality of choice for the evaluation of coronary artery disease and percutaneous coronary intervention (PCI). Both for clinical practice and research, there is a growing interest in 3-dimensional (3D) visualization, as this gives a more comprehensive and intuitively easier to understand representation, compared with 2-dimensional, cross-sectional images. Integrating 3D-IVOCT with classic X-ray angiographic images offers additional advantages and the prospect of integrating IVOCT in fluoroscopic guidance during PCI. Different vendors of IVOCT technology already provide integrated 3D rendering software in their consoles, making 3D images available at the 'push-of-a-button'. In this review, we will discuss (1) the basic principles and elaboration of 3D-IVOCT in recent years, (2) the feasibility and potential advantages of co-registration with X-ray angiography, (3) the currently available solutions for 3D imaging and their potential clinical applications, and (4) the ongoing development of applications for advanced 3D visualization.

Keywords Intravascular optical coherence tomography · 3-dimensional imaging · X-ray angiographic co-registration

This article is part of the Topical Collection on *Intravascular Imaging*

D. De Cock · T. Adriaenssens (✉)
Department of Cardiovascular Medicine, University Hospitals Leuven, B-3000Herestraat 49-3000, Leuven, Belgium
e-mail: tom.adriaenssens@uzleuven.be

S. Tu
Department of Radiology, Division of Image Processing, Leiden University Medical Center, Leiden, The Netherlands

G. J. Ughi · T. Adriaenssens
Department of Cardiovascular Sciences, Katholieke Universiteit Leuven, Leuven, Belgium

Introduction

Two-dimensional intravascular optical coherence tomography (2D-IVOCT) is a near infrared light-based imaging modality with an unrivalled spatial resolution. It has enhanced our understanding of atherosclerotic coronary artery disease tremendously and became the imaging modality of choice for the assessment of intracoronary stent implantation and atherosclerosis.

While first-generation time-domain OCT (TD-OCT) suffered from a low frame rate and long acquisition times, the introduction of frequency-domain OCT (FD-OCT) simplified the use of this imaging method in clinical practice [1, 2]. With current commercially available FD-OCT systems, it is possible to acquire a pullback within seconds, during the injection of a single bolus of contrast dye in the coronary artery, with a frame rate as high as 160–180 frames/s. Since the first-in-man experience with FD-OCT systems in 2008, the possibility to render 3D-reconstructions from these OCT acquisitions has been reported [1, 3]. Its potential value in assessing the true anatomic extent of coronary lesions, guiding complex percutaneous coronary interventions (PCI), and assessing stent failure has been emphasized in recent publications [4–7, 8••, 9, 10••].

While 2D-IVOCT is increasingly being used in routine clinical practice, 3-dimensional intravascular optical coherence tomography (3D-IVOCT) does not seem to find its way into every day cathlab routine. The need for long-time manual processing and off-line creation of 3D reconstructions was, until recent, the main limitation for this technology to be used. To acquire detailed, high-resolution 3D images, manual identification of the structures of interest (eg, guide-wire, stent strut, calcifications) on the 2D cross-sectional images was needed, making this a labor intensive and time-consuming procedure unsuitable for on-line application during PCI or for large scale use in clinical trials [8••]. Furthermore, as the

2D-IVOCT images are acquired along the line of the imaging catheter, 3D views will per definition align along a straight line, not respecting the angulation, bends, or tortuosity of the coronary vessel. Integrating 3D-IVOCT data into the 'luminogram' acquired with coronary CT or X-ray coronary angiography has the potential to generate anatomically correct, detailed images in various clinical scenarios in vivo [11••, 12].

Against this background, we will discuss 3D-IVOCT processing and imaging, as well as 3D-IVOCT co-registration with X-ray coronary angiography. We will discuss different methodologies described so far and focus in particular on recently developed rapid and fully automatic software algorithms. Examples of 3D-IVOCT visualization, including their potential clinical utility during PCI or for research purposes, will be highlighted.

3D IVOCT Imaging

3D-IVOCT Acquisition, Processing, and Visualization

3D-IVOCT images can be obtained through standard techniques for volume rendering. Many DICOM viewer software (commercially available or open source) can be used for this purpose, typically based on data processing using vtk/itk or similar libraries [13–16]. The most widely used software for this purpose is OsiriX (OsiriX foundation, Geneva, Switzerland), Intage Realia (Cybernet Systems, Co., Ltd, Tokyo, Japan) and the ones specifically developed by St. Jude Medical (St. Paul, MN) and Medis Special (Leiden, The Netherlands). Other companies (eg, Terumo Corp., Tokyo, Japan) are known to be working on their own software, which may be available soon. However, in general, many other different approaches can be successfully applied and there is no particular recommendation at this time of using one software with respect to another. Moreover, predefined color settings, illumination, and shading may be significantly different. This makes comparison between 3D rendering from different software rather difficult, especially with regard to its use in clinical studies. As a lot of work is done for the standardization of 2D-IVOCT and large consensus exists on optimal guidelines for conventional 2D-IVOCT visualization and validation [17], a lot of work remains to be done for its 3D counterpart by the IVOCT community. This would allow for more consistent 3D-IVOCT visualizations between different vendors and research groups, and more importantly guarantee minimum requirements and validation of different 3D-IVOCT applications to cardiovascular imaging (eg, lumen visualization, stent assessment, assessment of plaque distribution, and other advanced visualizations).

Visualization of 3D images is not only dependent on image processing and viewer software. Optimal acquisition of the 'source' OCT pullback may influence 3D imaging to an even greater extent. There is an inevitable trade-off between pullback speed, image resolution, and motion artifacts. A slower pullback speed and a longer acquisition time for a similar pullback length, gives rise to a higher incidence of motion artifacts (cardiac motion, relative motion of the imaging catheter to the vessel wall, etc), leading to elongation, rotation, or repetition of segments along the longitudinal axis. With fast pullback speeds, the incidence of motion artifacts is reduced, however, at the expense of a lower longitudinal resolution, giving a 'grainy' or even 'blurry' appearance to the 3D IVOCT reconstruction [18••]. In our opinion, the minimum requirements for a sufficient 3D image quality, is a longitudinal resolution as high as 10 frames per mm pullback (ie, a slice thickness of 0.1 mm). While with the previously commercially available C7 XR FD-OCT Imaging system by St.-Jude Medical (St. Paul, MN, USA), the pullback speed had to be reduced to 10 mm/sec to obtain a longitudinal resolution of 10 cross-sections per millimeter, the current Ilumien Optis system from the same vendor (with a frame rate of 180/sec) has a default setting of 18 mm/sec for the same longitudinal resolution. In the Terumo OFDI system (with a frame rate of 160/sec) a pullback speed of 20 mm/s corresponds to 8 frames per mm pullback (ie, a slice thickness of 0.125 mm). Also here, standardization on minimum requirements for acquisition by IVOCT experts, in order to obtain sufficient image resolution for 3D rendering, would be of interest for interventional cardiologists planning to use these modalities in clinical practice and for future research efforts with 3D-IVOCT evaluation of new techniques and devices.

While current literature on 3D-IVOCT is limited to case presentations, feasibility studies, and small series by different groups, some consistency regarding the nomenclature for 3D reconstructions can be found in most publications. In general, a 3D reconstruction is rendered as a *'longitudinal view'* from a 2D-IVOCT dataset, which is basically an external view from outside of the vessel. *'Cut-away views'* of the vessel down the longitudinal axis show the internal lumen of the segment of interest from externally to the vessel by removing a part of the reconstructed vessel wall. Internal views of the vessel looking either downstream (from proximal to distal) or upstream (from distal to proximal) along the longitudinal axis are generally referred to as *'fly-through views'*. In most cases, these views are complementary, showing the specific focus or problem of the interrogated coronary segment in different ways.

Vessel Morphology Visualization

The most easy and first clinical application of 3D-IVOCT was the assessment of vessel morphology and lumen narrowing. Compared with 2D-IVOCT images, 3D rendering gives a more intuitive and easy to interpret representation of lumen narrowing and lesion extension. For this purpose, no specific

processing (eg, image segmentation) of 2D-IVOCT images is required. Such basic visualizations can be obtained by 3D rendering of cross-sectional IVOCT images as they are acquired, using some specific color map, shading and illumination by adjusting the windowing level (ie, dynamic range and noise level) for optimal visualization. An example of such basic 3D-rendering (obtained without any data post-processing) is illustrated in Fig. 1. In some cases, vessel morphology can also be depicted through automatic segmentation of the vessel lumen border, displaying lumen contour (ie, a tubular structure) only. In both cases, qualitative and quantitative analysis of the vessel contour may allow for an easier identification of minimal lumen area across the entire IVOCT dataset. Currently, a basic 3D visualization for the assessment of vessel lumen morphology is available on the Illumien Optis OCT system (St. Jude Medical, St. Paul, MN), which can be used on-line during PCI (an example is given in Fig. 2). Furthermore, algorithms for fully automatic lumen segmentation are currently available and can be used on-line after data acquisition.

Stent and Guide-Wire Visualization

One of the most significant and broadly investigated applications of IVOCT is the visualization of intracoronary stents. Several publications pointed to the fact that 3D-IVOCT visualization has several advantages over conventional 2D image representation [1, 3, 8••, 19, 20]. The major pitfall of 3D visualization of stented segments in these first reports is that image preparation had to be done manually. To apply 3D-IVOCT to stent assessment, each stent strut, as well as the guidewire and the imaging catheter had to be manually identified in every 2D cross-sectional image. This manual segmentation of stent struts required a long processing time (2–5 hours as an IVOCT pullback typically contains >200 images), which is not suitable for on-line use during PCI making automated methods required for this application [1, 3].

The feasibility of on-line 3D-IVOCT reconstructions applying automatic stent struts segmentation has recently been demonstrated [18••, 21–24]. The aim of stent visualization in 3D is to highlight struts over the vessel wall surface. As such, automated 3D visualization of intracoronary stents can be obtained in 2 different ways: (1) IVOCT images can be processed for automatic stent strut and guide-wire segmentation (Fig. 3a and c) [18••, 21–23], or [2] 3D rendering can be directly applied to raw IVOCT images, by applying a specific colormap to enhance stent visualization (Fig. 3b). The latter approach has the advantage of not requiring any complex segmentation algorithm; the first approach has the advantage of depicting and better highlighting the structures of interest. Moreover, using a segmentation algorithm allows for more advanced automatic quantification, such as the identification of stent malapposition [24]. Importantly, in both cases, the processing time needs to be as quick a possible (including both automatic processing time and manual interactions) for being of value during a PCI procedure. Some vendors (eg, QAngioOCT Medis Specials bv., Leiden, The Netherlands) already commercialized dedicated software for

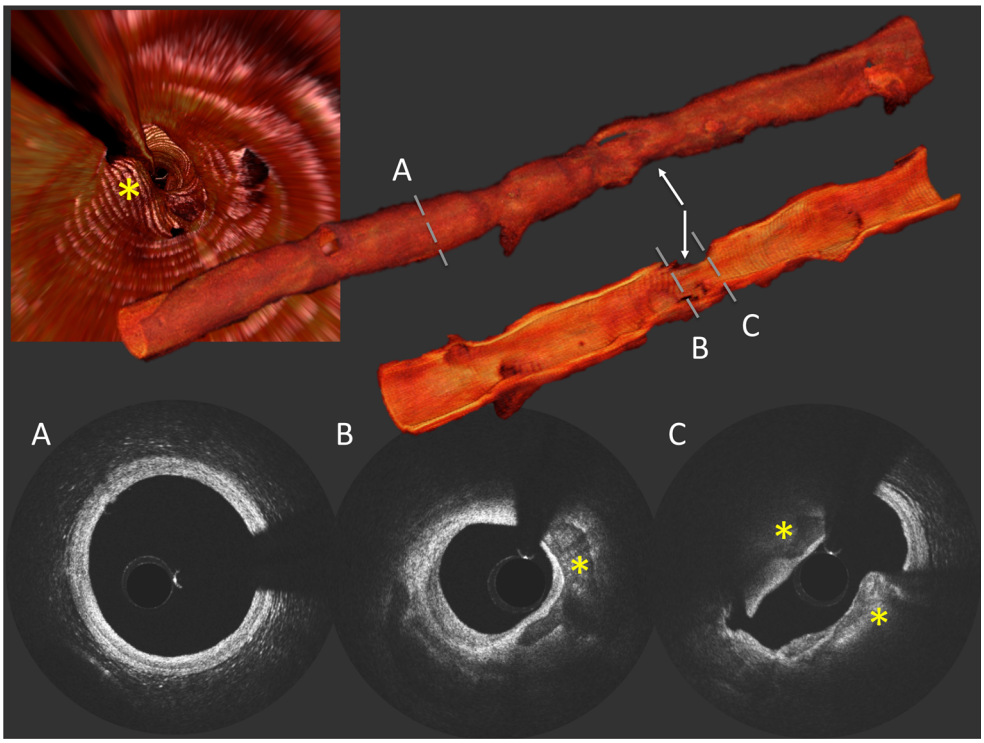

Fig. 1 3D rendering of a coronary artery lesion with non-occlusive lumen narrowing due to a calcified plaque (white arrows). 3D rendering gives an easy-to-interpret representation of the location of the lumen narrowing and the total extension of the lesion. A calcified lesion (yellow asterisk) can be observed in cross-sectional images (B) and (C); normal lumen size can be seen in cross-sectional image (A). Top-left image is a fly-through of the vessel visualizing the lesion from a few millimeters away. 3D renderings were obtained using OsiriX software (OsiriX Foundation, Geneva, Switzerland)

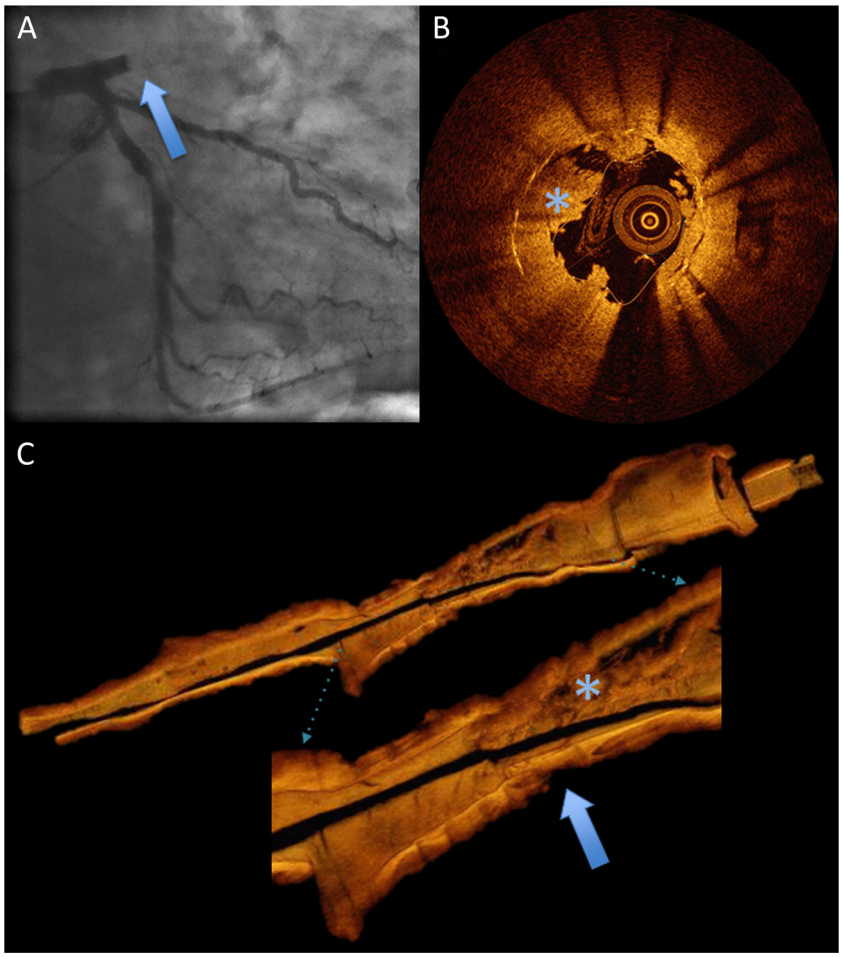

Fig. 2 Example of 3D-IVOCT rendering obtained using St. Jude Medical Ilumien Optis (St. Paul, MN, USA) visualization software. The 3D-IVOCT image gives an immediate picture of the vessel and lumen morphology easily identifying the culprit lesion (blue arrows). In this case, 3D-IVOCT is used to visualize an example of stent thrombosis as confirmed by the 2D image. The thrombus and its longitudinal extension is clearly visible from the 3D visualization (blue asterisks)

3D stent visualization. Moreover, Terumo Inc. (Tokyo, Japan) will soon release software integrated in the Terumo OFDI system for on-line, high-quality 3D rendering with automatic stent enhancement, available at the 'push-of-a-button' (Fig. 4). At the same time, multiple research groups have developed and are currently using their own prototypes and methods [18••, 21–24].

Recent studies showed that 3D stent rendering holds potential for the optimization of PCI procedures, such as bifurcation lesions [10••, 20, 25]. 3D-IVOCT has the capability of visualizing stent cells covering a side branch and visualizing guide-wires, allowing for an optimal rewiring of the side branch through a distal stent cell (Fig. 5). 2D-IVOCT images alone may be very difficult to interpret for the analysis of optimal rewiring and 3D visualization provides unique information for the optimization of such complex PCI procedures. Examples of the use of 3D-IVOCT for a bifurcation intervention are illustrated in Fig. 6. In a very recent study, Okamura et al showed that it is feasible to optimize side branch opening by guiding distal cell recrossing using 3D imaging on-line (ie, during the procedure). Moreover, it was observed that in cases where a connector between the rings of the stent was overlying the carina (which is impossible to detect with 2D-IVOCT), a higher incidence of floating and jailing struts was present after kissing balloon inflations, despite distal cell recrossing [10••]. The latter finding remarkably resembles the results of computer models, previously used to evaluate the behavior of current stents with open cell design in case of provisional side branch stenting [26]. Instead of only looking at the distal cell to recross, automatically delineating the stent cell with maximal sidebranch access, could further improve the practice of bifurcation PCI [27•]. Identifying or even color-coding the most distal stent cell with maximal unsupported side branch access, could then hypothetically be integrated on-line in the angiographic images using fusion techniques, guiding the operator towards 'the' cell to recross.

3D-IVOCT imaging can also be of particular use in determining the mechanisms of stent failure in vivo. Several studies describing 2D-IVOCT findings in patients suffering from stent thrombosis or in-stent restenosis have been published in the last years, focusing on the major added value of intracoronary imaging in elucidating pathophysiological mechanisms and guiding repeat revascularization [20–26, 27•, 28–30]. Some specific and complex stent-related

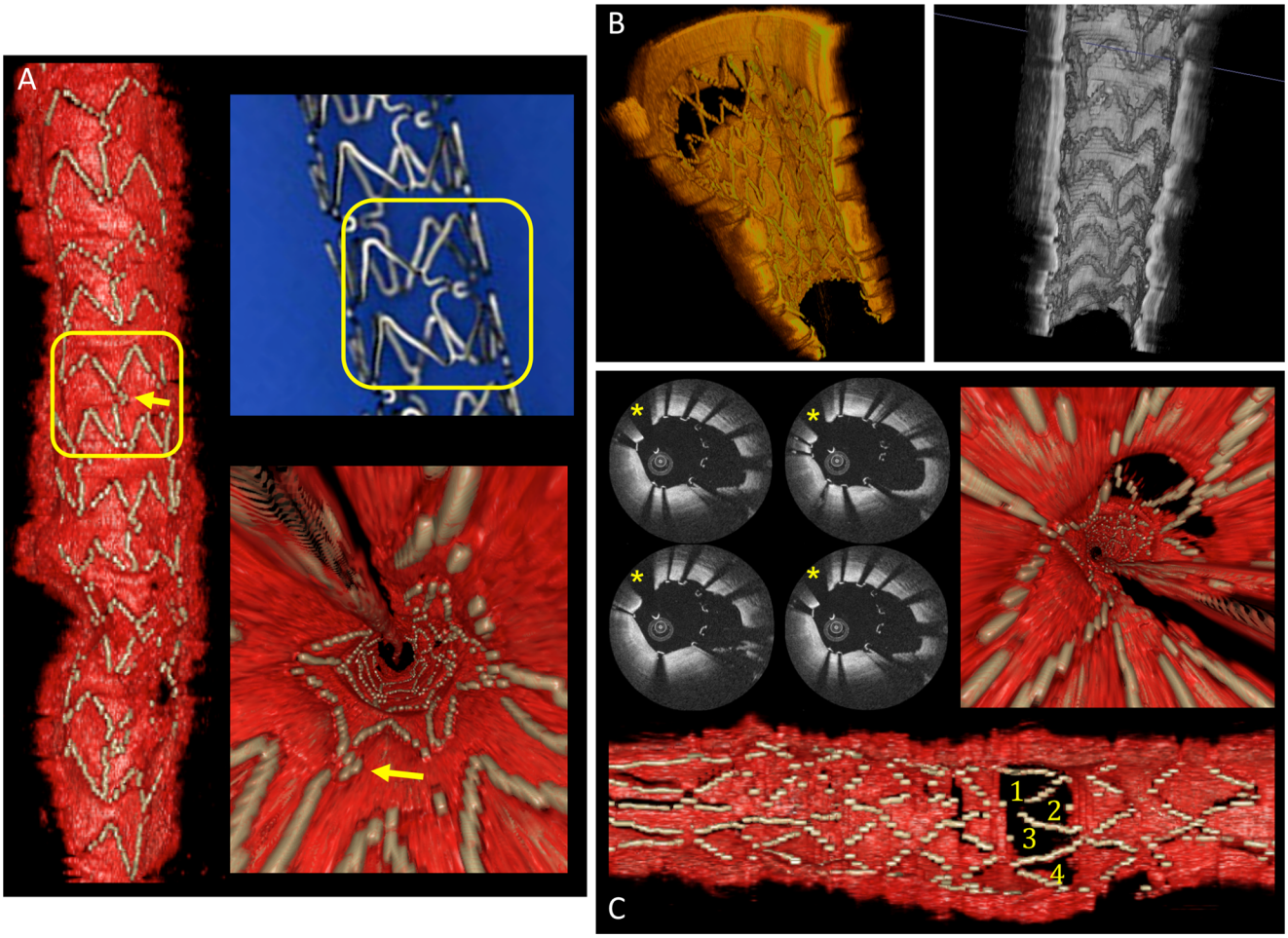

Fig. 3 3D visualization of coronary stents. Figures (A) and (C) show 2 examples of 3D stent visualization following fully-automatic stent strut segmentation (no manual correction of segmentation results was applied). Figure (B) was obtained without any image segmentation, using a specific color map for stent enhancement (QAngioOCT Medis Specials bv., Leiden, The Netherlands). Figures (A) and (C) are reprinted with permission from Optics Infobase (The Optical Society): Ughi GJ, Adriaenssens T, Desmet W, et al. Fully automatic 3-dimensional visualization of intravascular optical coherence tomography images: methods and feasibility in vivo. Biomed Optics Express. 2012;3:3291–303 [18••]

problems, remain, however, difficult to visualize if only 2D images are available. 3D-IVOCT offers unique insights in phenomena like stent fracture and stent deformation (Fig. 7) [31, 32]. As these mechanisms for stent failure often remain undetected, it could be of value to include routine 3D visualization in future registries on stent thrombosis and restenosis, using OCT.

Plaques and Other Advanced 3D IVOCT Methods and Applications

In addition to lumen and stent strut visualization, IVOCT is capable of assessing atherosclerosis in detail, giving important information about plaque composition and morphology. As such, 3D-IVOCT rendering techniques have been used for the visualization of atherosclerotic plaques and intracoronary thrombus [33]. This kind of representation gives very detailed information on longitudinal plaque distribution (eg, abundance of calcified plaques) and can potentially be used for the optimization of PCI procedures. Similarly, 3D visualization of tissue and plaque morphology can be merged with the visualization of stents. As recent publications point towards the importance of detecting neointimal changes for predicting recurrent events following PCI, 3D-IVOCT imaging might play a role in elucidating mechanisms of stent failure, such as neoatherosclerosis [34].

Plaque assessment, however, requires complex processing of IVOCT images that is typically done by an expert image reader, interpreting images in a qualitative way [35]. Although this approach can result in a very detailed 3D visualization, it is not suitable for on-line applications as it can only be applied post hoc. Recently, more advanced methods for automated plaque analysis have been developed. Algorithms for the semi-automated assessment of the thickness of the cap overlying a lipid core for the identification of thin-cap fibroatheroma (TCFA) have been presented (Fig. 8) [36•], as

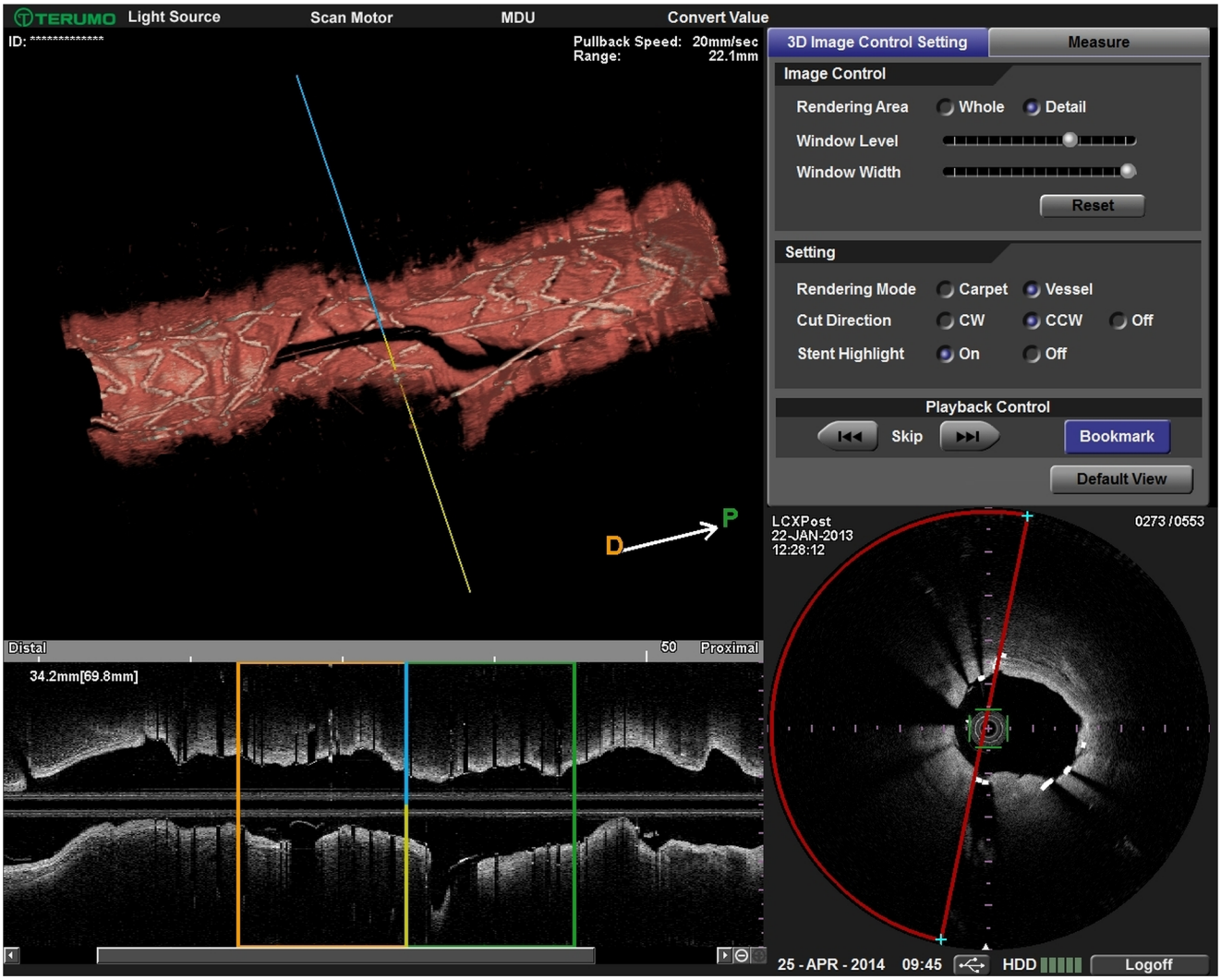

Fig. 4 Screenshot of the 3D rendering software integrated in the Terumo Lunawave OFDI system. The software allows to automatically highlight the coronary stent (copper color) on the top of the vessel (red color). Stent struts are segmented fully-automatic through the entire dataset. In the example, a freshly implanted stent is analyzed and visualized. The guidewire is also visible and depicted using the same color as the stent struts (ie, copper). This software will be integrated in the commercially available console and review station shortly. Courtesy of Terumo Inc. (Tokyo, Japan) with permission

well as approaches for the automatic detection of calcified and lipid-rich plaques (Fig. 9) [37, 38]. Automatic plaque characterization can be of value for advanced on-line 3D visualization, but currently presents several limitations. Compared with stent strut and lumen segmentation, automatic tissue analyses are more difficult to validate (as they require a large amount of matched histologic data) and are intrinsically more sensible to image artifacts. Moreover, a fully automatic framework (limiting or eliminating the need of user inputs) for this purpose, resulting in a short processing time suitable for on-line use may be difficult to achieve with current technology. In a future perspective, further developments in IVOCT technology for an enhanced detection of plaques and vessel inflammation, reducing intra- and inter-operator variability and improving IVOCT sensitivity and specificity, may help for an improved automatic analysis and subsequent 3D imaging of coronary atherosclerosis. Some examples of advanced modalities under research include multimodality imaging, such as combining IVOCT with near infrared fluorescence (OCT-NIRF) [39] or near-infrared spectroscopy (OCT-NIRS) [40].

Another application of IVOCT is the detection of stent strut malapposition and the assessment of neointimal coverage and thickness. These features have become important endpoints in clinical trials assessing the efficacy and safety of new and improved coronary stent designs [41–43]. Moreover, the detection of malapposition is of value for acutely optimizing the result of stent implantation [44]. Clinical studies, using coverage and malapposition at follow-up as an endpoint are, however, solely based on 2D-IVOCT assessment and only report the number and percentage of malapposed or uncovered

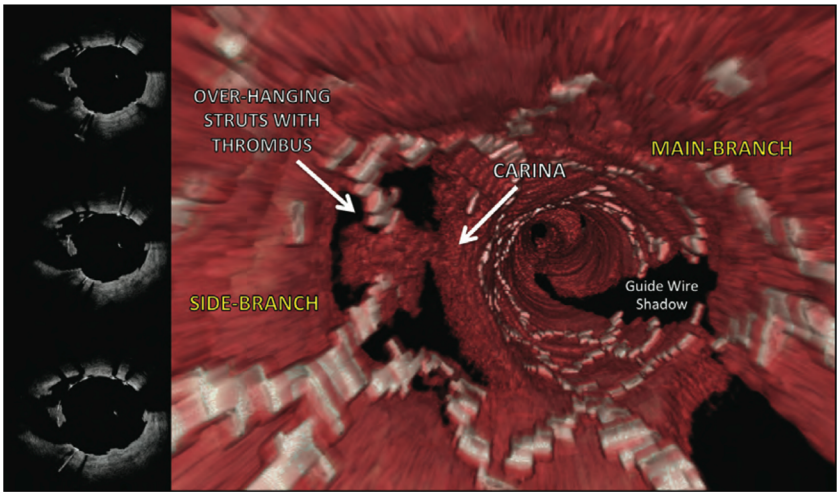

Fig. 5 An example of 3D IVOCT for the visualization of a stent overlying a side-branch (vessel wall is depicted in red and the stent struts in silver color). The main vessel, the side branch and the carina are clearly depicted by 3D-IVOCT. Both 2D and 3D images show thrombus above struts overlying the side branch, however, 3D visualization better depicts stent cells. Stent struts were manually segmented preparing images for 3D by an expert image reader. Reprinted with permission from Oxford Journals: Farooq V, Gogas BD, Okamura T, et al. Three-dimensional optical frequency domain imaging in conventional percutaneous coronary intervention: the potential for clinical application. Eur Heart J. 2013;34:875–85. [8••]

struts per stented segment, lacking detailed information on the spatial distribution of these findings. Moreover, analyzing pullbacks of stented segments frame-by-frame is a time-consuming activity and, in general, cross-sections are

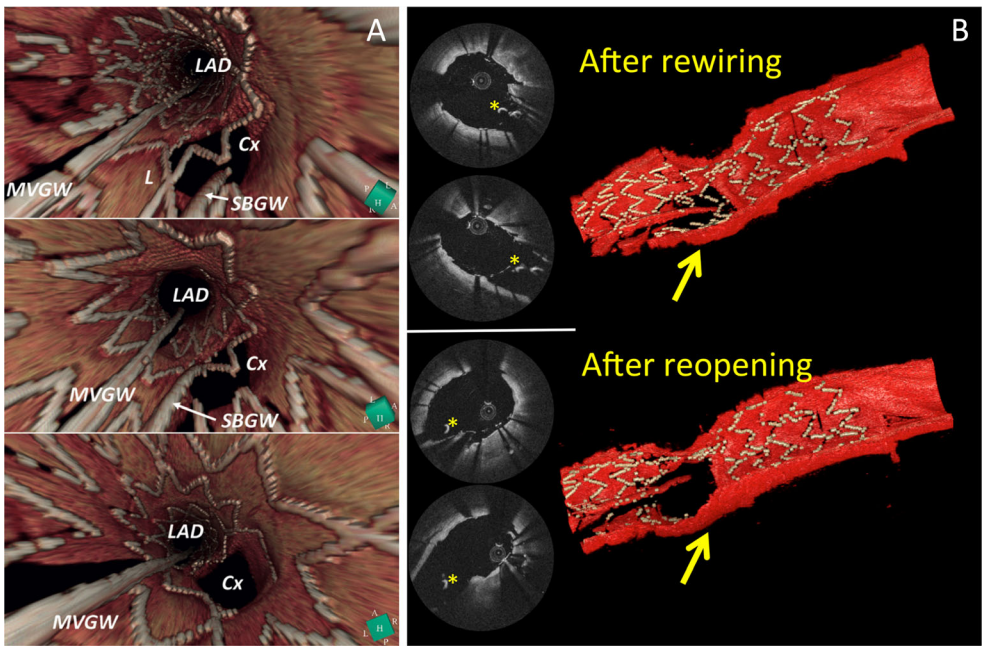

Fig. 6 Examples of the use of 3D IVOCT to guide bifurcation intervention. Panel A shows an example of rewiring to the circumflex artery (Cx). Top image illustrates the first attempt of rewiring, where the side-branch guidewire (SBGW) is passing through a proximal cell. Middle image illustrates the second attempt, with correct rewiring through the distal cell. Bottom image shows good result after kissing balloon inflations with no free floating stent struts at the ostium of the Cx. Panel B shows a similar example of rewiring through an optimal, distal cell. Images in Panel A were obtained through manual segmentation of stent struts off-line, while images in panel B were rendered through fully-automatic segmentation and 3D rendering using dedicated software. Panel A is reprinted with permission from Europa Digital & Publishing: Okamura T, Onuma Y, Yamada J, et al. 3D optical coherence tomography: new insights into the process of optimal rewiring of side branches during bifurcational stenting. EuroIntervention. 2014; [Epub ahead of print]. [10••]. Panel B is reprinted with permission from Optics Infobase (The Optical Society): Ughi GJ, Adriaenssens T, Desmet W, et al. Fully automatic 3-dimensional visualization of intravascular optical coherence tomography images: methods and feasibility in vivo. Biomed Optics Express. 2012;3:3291–303. [18••]

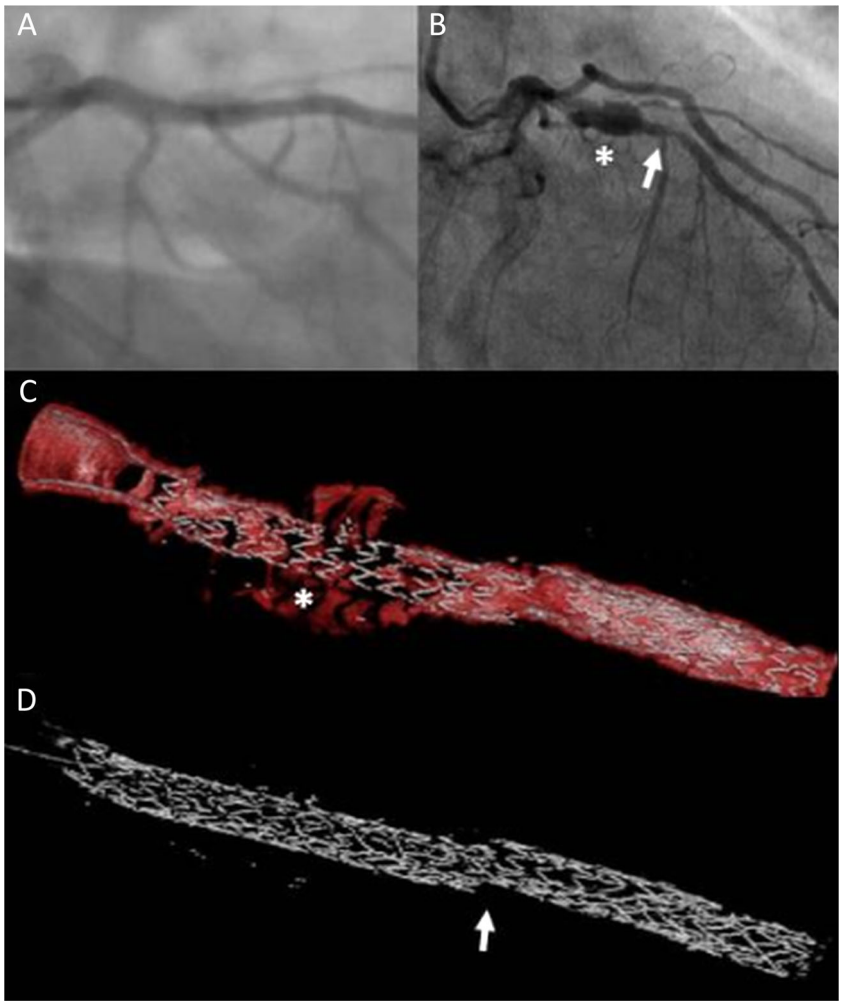

Fig. 7 3D visualization of a stent fracture in-vivo. The angiographic result immediately after PCI is satisfactory (panel A), while a coronary aneurysm (asterisk) and a tight stenosis (withe arrow) can be noted in the stented segment at follow-up coronary angiography (panel B). 3D-IVOCT visualization, after off-line segmentation using an automated software algorithm, shows severe acquired malapposition at the level of the coronary aneurysm (panel C, asterisk). A complete stent fracture is visible, especially when a colormap highlighting the stent is applied (panel D, arrow). 3D images were obtained with Intage Realia software (Cybernet Systems, Co., Ltd, Tokyo, Japan)

analyzed at intervals of 0.6–1 mm along the longitudinal axis. Different research groups developed automatic algorithms for the assessment of neointimal coverage over stent struts and stent strut malapposition, allowing for 3D visualization of clusters of malapposed and uncovered struts, as well as color-coded contour plots for visualization of specific patterns of neointimal growth [24, 45, 46]. These advanced visualizations facilitate a time efficient quantification of neointimal

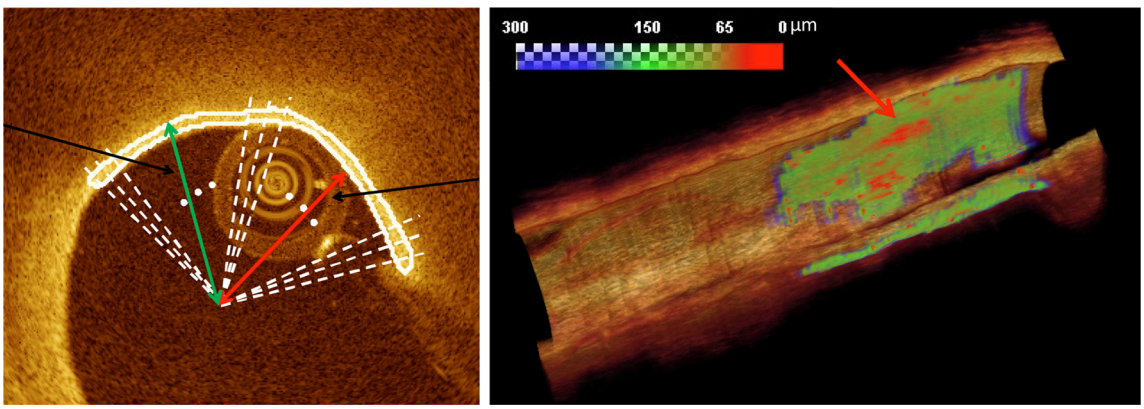

Fig. 8 3D visualization of lipid plaque cap thickness. Cap thickness is obtained off-line, using a semi-automatic computer aided approach. The color map used to visualize cap thickness ranges from red (very thin cap, <65 µm) to green (>65 µm) and blue (>165 µm). Reprinted with permission from Optics Infobase (The Optical Society): Wang Z, Chamie D, Bezerra HG, et al. Volumetric quantification of fibrous caps using intravascular optical coherence tomography. Biomed Optics Express. 2012;3:1413–26. [36•]

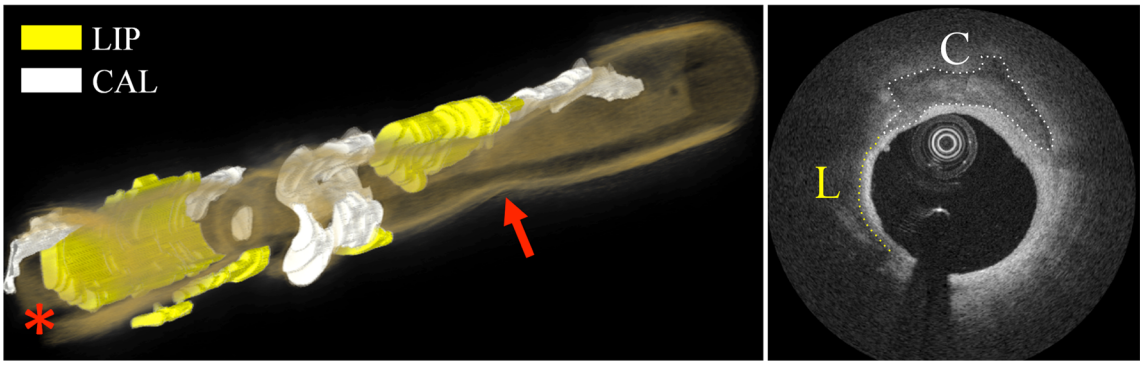

Fig. 9 3D visualization of lipid and calcified plaques over an entire vessel segment. Tissue characterization was obtained through an automatic algorithm. Red arrow is pointing to luminal narrowing. Reprinted with permission from Optics Infobase (The Optical Society): Ughi GJ, Adriaenssens T, Sinnaeve P, et al. Automated tissue characterization of in vivo atherosclerotic plaques by intravascular optical coherence tomography images. Biomed Optics Express. 2013;4:1014–30. [38]

coverage and the burden of malapposition, as well as their spatial distribution in 3 dimensions. Although these software applications are well-validated against conventional 2D assessment by expert readers, data on the clinical implications of detecting spatial clusters of uncovered and malapposed struts are lacking. Future research should focus on the relationship between OCT-detected characteristics of delayed vessel wall healing and late adverse events, such as stent thrombosis.

Co-Registration of 3D-IVOCT and Angiography

Under the condition that a motorized transducer pullback with constant speed is used in the intracoronary image acquisition, the rationale for the co-registration of X-ray angiography and intracoronary imaging is to use the spatial relationship between the vessel segment and the intracoronary pullback trajectory. Earlier approaches for co-registration between intracoronary IVUS and X-ray angiography [47, 48] can be applied to IVOCT co-registration. However, this approach would require the reconstruction of the OCT imaging catheter from 2 angiographic views, and assume it to be the pullback trajectory so that the OCT cross-sectional images can be aligned along the trajectory. This is not a trivial task in practice due to the difficulty in segmenting both the imaging catheter and the lumen from angiographic images, and the requirement of a second angiographic view showing the IVOCT catheter, which is often unavailable. Tu et al [49, 50••] proposed a rapid and straightforward on-line solution that could fit into current cathlab practice. Instead of segmenting and reconstructing the imaging catheter, the corresponding IVOCT cross-sectional image frame was estimated from the reconstructed angiographic centerline and a baseline position. This approach only requires the operator to reconstruct the angiographic centerline in 3D and register it with the IVOCT image pullback by indicating a baseline position in both imaging modalities. These baseline positions can be found in anatomic or mechanical landmarks visible in both angiographic and IVOCT images, such as a large bifurcation or a stent border. After determining these baseline positions, the markers superimposed on the angiographic views and the IVOCT pullback are synchronized. The interpretation of vessel dimensions becomes more comprehensive and the interventional cardiologist knows exactly where to position the stent under the guidance of conventional X-ray images. An example of combining 3-dimensional quantitative coronary angiography (3D-QCA) and IVOCT is given in Fig. 10. From the registered dataset, the same lesion is identified in both X-ray and IVOCT images. The quantifications from these 2 imaging modalities are seamlessly integrated. In this example, the target vessel is the LAD and has a minimum lumen diameter and minimum lumen area of 1.5 mm and 1.8 mm^2, respectively, as assessed by 3D-QCA, while the IVOCT measurements at the same position are 1.35 mm and 2.08 mm^2, respectively.

The feasibility of using co-registration online was recently investigated in the DOCTOR Fusion study [51]. This pilot clinical study demonstrated that on-line co-registration of X-ray angiography and IVOCT was successful in all analyzed cases. There was a significant discrepancy between operator-based and software-based co-registrations. Without using the co-registration software, the mean "Operator Registration Error", defined to quantify the cumulated numerical difference between operator-based and software-based co-registered stent border positions, was 5.4±3.5 mm. The operator implanted the stent blind to the software-based co-registration, resulting in a mean longitudinal geographic miss of 5.4± 2.6 mm between the co-registered stent border positions and the actual stent deployment border positions. Meanwhile, segments of the target lesion indicated on IVOCT were left uncovered by stent in 70 % of the study population [51]. These data imply that in routine clinical practice there might be significant error in translating the landing zones identified by IVOCT to the angiographic images. Applying co-

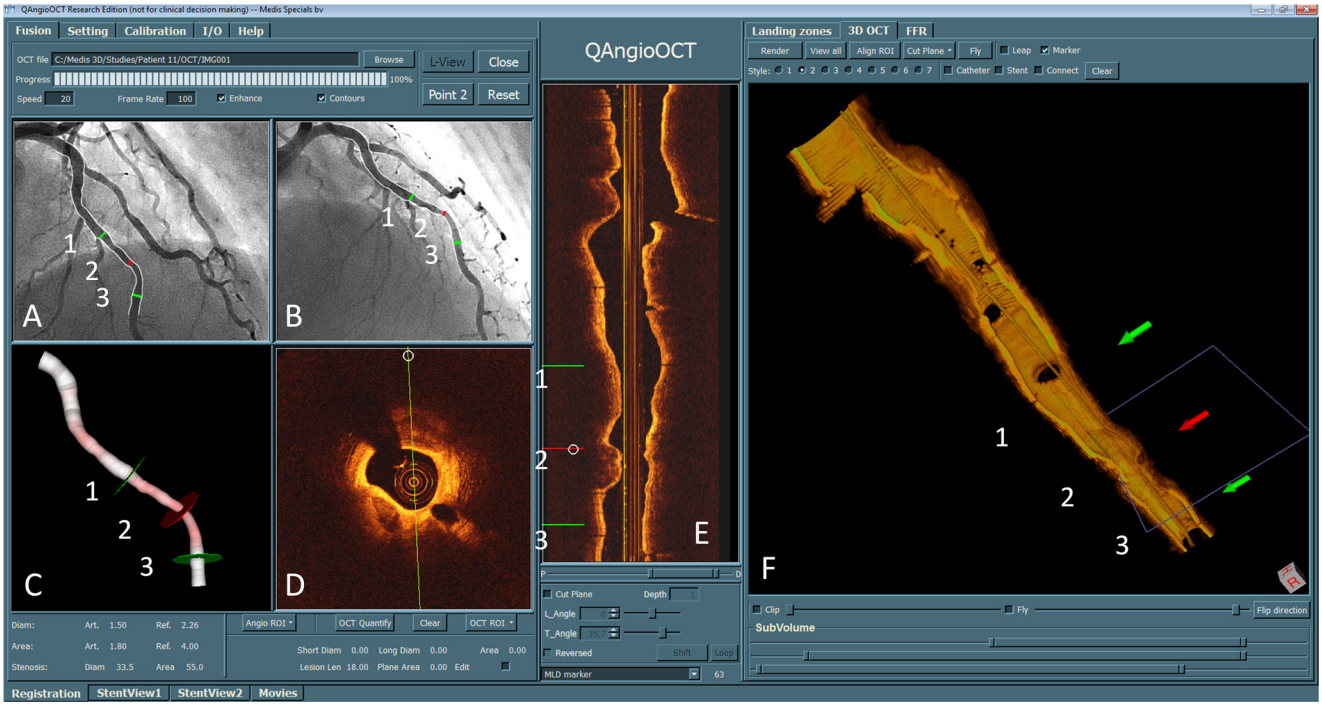

Fig. 10 Co-registration of X-ray angiography and optical coherence tomography. The 3 markers indicated by numbers in panel A, B, C, E, and F were synchronized after performing the co-registration. By default the 2 green markers (1 and 3) were positioned at the landing zones and the red marker was positioned at the most narrowed location. Courtesy of Medis Special (Leiden, The Netherlands)

registration during PCI might improve the accuracy of stent sizing and positioning, minimizing geographic miss.

Despite the fact that IVOCT provides accurate quantification regarding lumen size, certain artefacts, such as distortions caused by myocardial muscle contraction and oblique imaging (eg, the imaging catheter is not parallel to the arterial centerline) can influence quantification and interpretation. In the DOCTOR Fusion study, it was noted that cardiac motion causes a 10 mm of the same vessel segment to appear twice in an IVOCT image pullback [51]. In such case, the co-registration of X-ray angiography and IVOCT helps to identify the artefact and avoids inappropriate decision making. A recent study applying the co-registration software to compare the arterial lumen size by 3D-QCA and IVOCT demonstrated that the difference in lumen area by 3D-QCA and IVOCT tended to increase as lumen size increased and the interrogated vessel became more tortuous [50••]. Therefore, the integration of IVOCT and X-ray angiography might constitute a necessary step towards optimized PCI.

By aligning the in-plane angulation of the side branches between X-ray angiography and IVOCT, the IVOCT pullback could be reconstructed in a naturally bent shape and fused with the 3D angiographic reconstruction. Applying this fusion technique can overcome the limitation of IVOCT imaging not preserving vessel tortuosity information. In this way, high-resolution anatomic models can be generated for studies related to flow simulation and biomechanical response to implanted devices [12]. It is important to note that the fusion requires both longitudinal alignment and in-plane angulation alignment. While the co-registration provides corresponding information between the 3D angiographic centerline and the IVOCT image frames for the longitudinal alignment, an additional image processing step needs to be implemented for in-plane angulation alignment to correctly orient the IVOCT image frames in 3D space. This is difficult to validate in vivo. Tu et al proposed to use side branches in 3D to align the in-plane angulation. Although it requires the angiographic reconstruction of the side branches in 3D, it provides a direct and intuitive way to verify the correct angulation [11••, 12]. Figure 11 shows an example of 3D fusion of X-ray angiography and IVOCT after stent implantation in a coronary bifurcation. Using the 3D angiographic reconstruction as "road map", the OCT image pullbacks from the main vessel and from the side branch were merged in 3D, forming a high-resolution reconstruction of the interrogated bifurcation. This can be of particular interest in clinical research focusing on the use of dedicated devices for the treatment of complex coronary artery disease. The example given in Fig. 11 nicely demonstrates the conical shape of the dedicated AXXESS device for bifurcation treatment and its relation to the additionally implanted tubular stents in a so-called 'V-configuration'. Other dedicated devices for bifurcation lesions, such as the Tryton stent or complex two-stent techniques, such as the culotte and the crush technique, interplay in a complex 3-

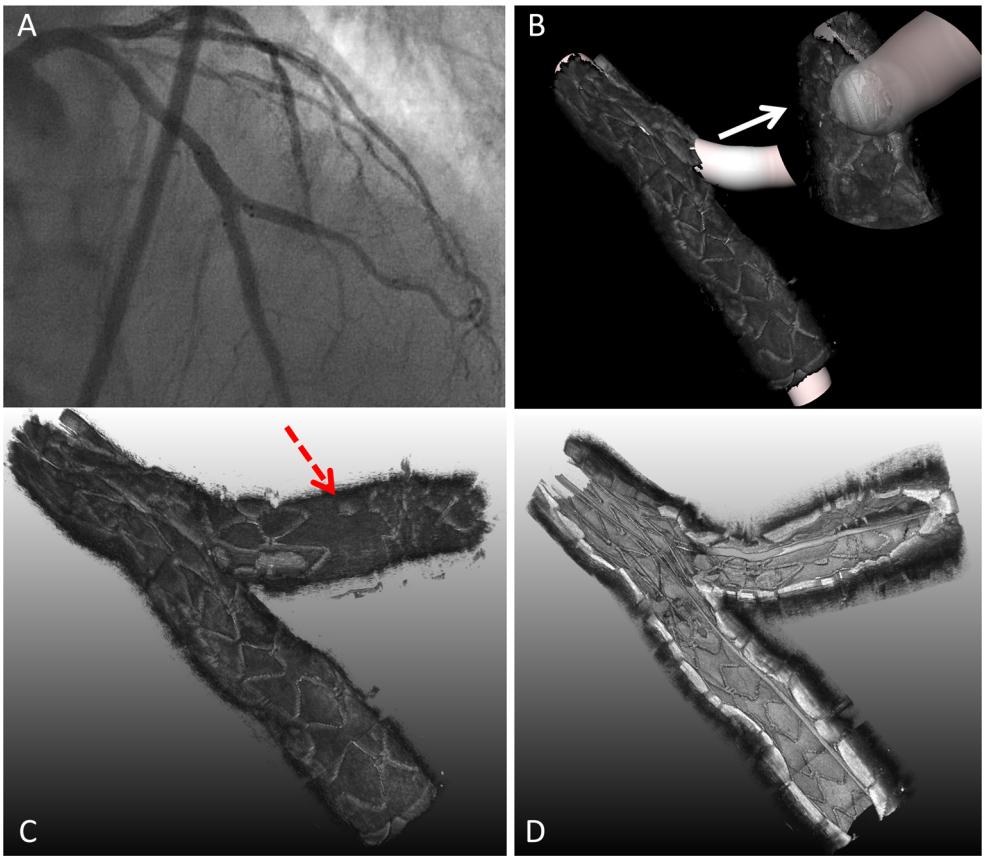

Fig. 11 Fusion of X-ray angiography and OCT for assessment of a bifurcation intervention. Panel **a** shows an angiographic projection after implantation of an AXXESS stent in the proximal main vessel and 2 BIOMATRIX stents in the distal main vessel and the side branch, respectively. In Panel **b**, fusion of the 3D angiographic reconstruction with the OCT pullback from the LAD is shown, with correct alignment of the diagonal branch in 3 dimensions. Panel C and D show the bifurcation reconstruction by merging the second OCT pullbacks from the diagonal branch. The red dashed arrow indicates the radiopaque marker of the BIOMATRIX stent implanted in the diagonal branch

dimensional way with the anatomy of the bifurcation lesion treated and with vessel morphology. Moreover, future studies in bifurcation treatment will focus on complex PCI techniques with the use of bioresorbable devices. Currently used imaging endpoints, such as coverage and apposition, measured on 2D images will lose their value, since the device itself will disappear over time. Volumetric assessment, flow simulation and biomechanical response to these 'scaffolds' will become important outcome measures, and it is to be expected that rapidly available 'fusion' images, as shown above, will gain importance in future studies.

Current Application and Perspectives for Future Development

Several leading experts in the field of IVOCT have underlined the fact that automatic 3D visualization would bring IVOCT closer to becoming a practical imaging technique in the cathlab [8••, 20]. Improvements in the hardware for image acquisition on the one hand, and further development of software for image processing and analysis on the other, are subjects of ongoing research.

Although the frame rate of commercially available IVOCT catheters has improved, still only 12 % of the lumen is sampled by the laser beam in the longitudinal direction. This longitudinal sampling interval of 250 μm largely exceeds the transverse resolution of IVOCT, which is approximately 30 μm. This is problematic for 3D-IVOCT applications, since undersampling in the longitudinal direction critically affects the accuracy of the visualizations. Wang et al recently described an ultrafast IVOCT system, consisting of a micromotor-based catheter and a dispersion compensated Fourier domain mode locked (FDML) laser [52•]. This technology allows for acquisition at 3200 frames per second, corresponding to a 100 mm/second pullback speed and a 30 μm longitudinal sampling interval, improving image quality in the longitudinal direction and showing the potential to acquire IVOCT data of a 5–7 cm vessel segment within 1 cardiac cycle. Moreover, IVOCT catheters incorporating a micromotor, compared with current cable-driven rotating catheters, will be less prone to motion artifacts (eg, relative motion of the imaging catheter to the vessel wall and nonuniform rotation distortion), further improving the accuracy of 3D rendering [53].

As mentioned before, basic 3D visualization for the assessment of vessel lumen morphology is available at the 'push-of-a button' in the commercially available Ilumien Optis system (St. Jude Medical, St. Paul, MN, USA) and other vendors will release similar software products soon. This basic 3D rendering can be used as a complimentary tool to standard 2D-IVOCT as it is intuitively easier to understand and provides

a global perspective, with subsequent targeted assessment in 2D cross-sections whenever necessary. Rapid improvement in software for automatic stent strut detection is made. This will further increase the added value of 3D-IVOCT imaging in daily practice, guiding stent optimization with postdilatation in case of malapposition or guiding complex PCI, such as bifurcation treatment. More research needs to be done on the validation of automated plaque characterization and dedicated quantitative software for the assessment of neointimal coverage, before these advanced applications can enter the clinical trial arena. In the long run, automatic co-registration of 3D-IVOCT with X-ray angiography could be seen as the ultimate goal. On the one hand, the unrivalled spatial resolution of OCT overcomes a number of limitations, inherent to classic coronary angiography. On the other hand, X-ray angiography adds to 3D-IVOCT in preserving vessel tortuosity information and may serve as a stent/vessel model further mitigating motion artefacts. In the electrophylsiologist community, 3D overlay imaging for mapping and guiding complex ablation procedures has become standard of care. It is conceivable that intravascular imaging modalities will be integrated directly into future X-ray systems in the coronary catheter laboratory.

Conclusions

While 2D-IVOCT has an important place in contemporary interventional cardiology and has become the image modality of choice for the assessment of stents in clinical studies, 3D-IVOCT has largely been confined to bench testing and the generation of appealing images and animations. In this review, we demonstrated that ongoing efforts by multiple research groups rapidly change this exciting new field in intracoronary imaging. With the development of fast and accurate software algorithms, providing high-quality 3D visualizations 'at the push-of-a-button', as well as the interest of commercial enterprises in incorporating 3D applications in their consoles, it is to be expected that in the near future 3D-IVOCT may play a substantiate role in clinical practice and change the imaging endpoints, currently defined in device-related research. The ongoing improvements in automated fusion of high-resolution IVOCT images with conventional X-ray angiography, will inevitably change the way we guide PCI in everyday clinical practice within the next 10 years.

Compliance with Ethics Guidelines

Conflict of Interest Shengxian Tu is employed by Medis Medical Imaging Systems BV. Dries De Cock, Giovanni J. Ughi, and Tom Adriaenssens declare that they have no conflicts of interest.

Human and Animal Rights and Informed Consent This article does not contain any studies with human or animal subjects performed by any of the authors

References

Papers of particular interest, published recently, have been highlighted as:

- • Of importance
- •• Of major importance

1. Tearney GJ, Waxman S, Shishkov M, et al. Three-dimensional coronary artery microscopy by intracoronary optical frequency domain imaging. JACC Cardiovasc Imaging. 2008;1:752–61.
2. Drexler W, Fujimoto JG. Optical coherence tomography: technology and applications. 1st ed. Massachusetts: Springer; 2008.
3. Farooq V, Okamura T, Gogas BD, et al. 3D reconstructions of optical frequency domain imaging to improve understanding of conventional PCI. JACC Cardiovasc Imaging. 2011;4:1044–6.
4. Okamura T, Onuma Y, García-García HM, et al. 3-Dimensional optical coherence tomography assessment of jailed side branches by bioresorbable vascular scaffolds: a proposal for classification. JACC Cardiovasc Interv. 2010;3:836–44.
5. Foin N, Viceconte N, Chan PH, et al. Jailed side branches: fate of unapposed struts studied with 3D frequency-domain optical coherence tomography. J Cardiovasc Med (Hagerstown). 2011;12:581–2.
6. Gogas BD, Farooq V, Onuma Y, et al. Three-dimensional optical frequency domain imaging for the evaluation of primary percutaneous coronary intervention in ST-segment elevation myocardial infarction. Int J Cardiol. 2011;151:103–5.
7. Ughi GJ, Dubois C, Desmet W, et al. Provisional side branch stenting: presentation of an automated method allowing online 3D OCT guidance. Eur Heart J Cardiovasc Imaging. 2013;14:715.
8. •• Farooq V, Gogas BD, Okamura T, et al. Three-dimensional optical frequency domain imaging in conventional percutaneous coronary intervention: the potential for clinical application. Eur Heart J. 2013;34:875–85. *This comprehensive paper gives a state-of-the-art review of the different clinical applications of 3D-IVOCT imaging. Furthermore, the paper is beautifully illustrated with excellent cases*.
9. Mestre RT, Alegria-Barrero E, Di Mario C. A coronary "tunnel": optical coherence tomography assessment after rotational atherectomy. Catheter Cardiovasc Interv. 2014;83:E171–3.
10. •• Okamura T, Onuma Y, Yamada J, et al. 3D optical coherence tomography: new insights into the process of optimal rewiring of side branches during bifurcational stenting. EuroIntervention. 2014;[Epub ahead of print]. *In this pilot trial, the feasibility of online 3D-IVOCT imaging for guiding provisional bifurcation treatment is demonstrated for the first time.*
11. •• Tu S, Holm NR, Christiansen EH, et al. First presentation of 3-dimensional reconstruction and centerline-guided assessment of coronary bifurcation by fusion of X-ray angiography and optical coherence tomography. JACC Cardiovasc Interv. 2012;5:884–5. *This study describes the methodology for co-registration of 3D quantitative coronary angiography with IVOCT pullbacks acquired from the different branches in a coronary bifurcation.*
12. Tu S, Pyxaras SA, Li Y, et al. In vivo flow simulation at coronary bifurcation reconstructed by fusion of 3-dimensional X-ray angiography and optical coherence tomography. Circ Cardiovasc Interv. 2013;6:e15–7.
13. Visualization Toolkit (VTK). Kitware Inc. Available at: http://www.vtk.org. Accessed April 8, 2014.

14. Rosset A, Spadola L, Ratib O. OsiriX: an open-source software for navigating in multidimensional DICOM images. J Dig Imaging. 2004;17:205–16.
15. 3D DICOM viewer INTAGE Realia. Cybernet Systems, CO., LTD. Available at: http://kgt.cybernet.co.jp/viz/realia/english/users_guide.html. Accessed: April 8, 2014.
16. MeVisLab - Medical Image Processing and Visualization. Available at: http://www.mevislab.de. Accessed: April 8, 2014.
17. Tearney GJ, Regar E, Akasaka T, et al. Consensus standards for acquisition, measurement, and reporting of intravascular optical coherence tomography studies: a report from the International Working Group for Intravascular Optical Coherence Tomography Standardization and Validation. J Am Coll Cardiol. 2012;59:1058–72.
18.•• Ughi GJ, Adriaenssens T, Desmet W, et al. Fully automatic three-dimensional visualization of intravascular optical coherence tomography images: methods and feasibility in vivo. Biomed Opt Express. 2012;3:3291–303. *In this publication, a novel method for automatic segmentation of cross-sectional IVOCT images allowing for advanced 3D visualization with stent enhancement is described. Different clinical applications of this method are beautifully illustrated.*
19. Kubo T, Tanaka A, Kitabata H, et al. Application of optical coherence tomography in percutaneous coronary intervention. Circ J. 2012;76:2076–83 *[Epub Jul 31, 2012]*.
20. Di Mario C, van der Giessen WJ, Foin N, et al. Optical coherence tomography for guidance in bifurcation lesion treatment. EuroIntervention. 2011;6(Suppl J):99–106.
21. Nakao F, Ueda T, Nishimura S, et al. Novel and quick coronary image analysis by instant stent-accentuated three-dimensional optical coherence tomography system in catheterization laboratory. Cardiovasc Interv Ther. 2013;28:235–41.
22. Lu H, Gargesha M, Wang Z, et al. Automatic stent detection in intravascular OCT images using bagged decision trees. Biomed Opt Express. 2012;3:2809–24.
23. Tsantis S, Kagadis GC, Katsanos K, et al. Automatic vessel lumen segmentation and stent strut detection in intravascular optical coherence tomography. Med Phys. 2012;39:503–13.
24. Adriaenssens T, Ughi GJ, Dubois C, et al. Automated detection and quantification of clusters of malapposed and uncovered intracoronary stent struts assessed with optical coherence tomography. Int J Cardiovasc Imaging. 2014;30:839–48.
25. Gutierrez-Chico JL, Alegria-Barrero E, Teijeiro-Mestre R, et al. Optical coherence tomography: from research to practice. Eur Heart J Cardiovasc Imaging. 2012;13:370–84.
26. Gastaldi D, Morlacchi S, Nichetti R, et al. Modelling of the provisional side-branch stenting approach for the treatment of atherosclerotic coronary bifurcations: effects of stent positioning. Biomech Model Mechanobiol. 2010;9:551–61.
27.• Wang A, Eggermont J, Dekker N, et al. 3D assessment of stent cell size and side branch access in intravascular optical coherence tomographic pullback runs. Comput Med Imaging Graph. 2014;38:113–22. *In this paper, a methodology for quantification of stent cell area overlying a side branch is described in a phantom model. Automatic quantification and detection of maximal side branch access can be important for better guiding bifurcation intervention in the future.*
28. Parodi G, La Manna A, Di Vito L, et al. Stent-related defects in patients presenting with stent thrombosis: differences at optical coherence tomography between subacute and late/very late thrombosis in the Mechanism Of Stent Thrombosis (MOST) study. EuroIntervention. 2013;9:936–44.
29. Kang SJ, Mintz GS, Akasaka T, et al. Optical coherence tomographic analysis of in-stent neoatherosclerosis after drug-eluting stent implantation. Circulation. 2011;123:2954–63.
30. Gonzalo N, Serruys PW, Okamura T, et al. Optical coherence tomography patterns of stent restenosis. Am Heart J. 2009;158:284–93.
31. Kim S, Kim CS, Na JO, et al. Coronary Stent Fracture Complicated Multiple Aneurysms Confirmed By 3-Dimensional Reconstruction Of Intravascular-Optical Coherence Tomography In A Patient Treated With Open-Cell Designed Drug-Eluting Stent. Circulation. 2014;129:E24–7.
32. Hiltrop N, De Cock D, Ferdinande B, et al. Detailed in vivo visualization of stent fracture causing focal restenosis using 3D reconstruction software for high-resolution optical coherence tomography images. Eur Heart J Cardiovasc Imaging. 2014;15(6):714 *[Epub ahead of print]*.
33. Waxman S, Freilich MI, Suter MJ, et al. A case of lipid core plaque progression and rupture at the edge of a coronary stent: elucidating the mechanisms of drug-eluting stent failure. Circ Cardiovasc Intervent. 2010;3:193–6.
34. Ughi GJ, Steigerwald K, Adriaenssens T, et al. Automatic characterization of neointimal tissue by intravascular optical coherence tomography. J Biomed Opt. 2014;19:21104.
35. Yabushita H, Bouma BE, Houser SL, et al. Characterization of human atherosclerosis by optical coherence tomography. Circulation. 2002;106:1640–5.
36.• Wang Z, Chamie D, Bezerra HG, et al. Volumetric quantification of fibrous caps using intravascular optical coherence tomography. Biomed Opt Express. 2012;3:1413–26. *This publication describes the methodology for automatic quantification of the cap thickness in lipid-rich plaques, allowing for 3D visualization of the characteristics and the extent of thin-cap fibroatheromas in vivo*.
37. Van Soest G, Goderie T, Regar E, et al. Atherosclerotic Tissue Characterization In Vivo By Optical Coherence Tomography Attenuation Imaging. J Biomed Opt. 2010;15:011105.
38. Ughi GJ, Adriaenssens T, Sinnaeve P, et al. Automated tissue characterization of in vivo atherosclerotic plaques by intravascular optical coherence tomography images. Biomed Opt Express. 2013;4:1014–30.
39. Yoo H, Kim JW, Shishkov M, et al. Intra-arterial catheter for simultaneous microstructural and molecular imaging in vivo. Nat Med. 2011;17:1680–4.
40. Fard AM, Vacas-Jacques P, Hamidi E, et al. Optical coherence tomography—near infrared spectroscopy system and catheter for intravascular imaging. Opt Express. 2013;21:30849–58.
41. Bezerra HG, Costa MA, Guagliumi G, et al. Intracoronary optical coherence tomography: a comprehensive review clinical and research applications. JACC Cardiovasc Interv. 2009;2:1035–46.
42. Prati F, Regar E, Mintz GS, et al. Expert review document on methodology, terminology, and clinical applications of optical coherence tomography: physical principles, methodology of image acquisition, and clinical application for assessment of coronary arteries and atherosclerosis. Eur Heart J. 2010;31:401–15.
43. Guagliumi G, Sirbu V. Optical coherence tomography: high resolution intravascular imaging to evaluate vascular healing after coronary stenting. Catheter Cardiovasc Interv. 2008;72:237–47.
44. Allahwala UK, Cockburn JA, Shaw E, et al. Clinical utility of optical coherence tomography (OCT) in the optimisation of Absorb bioresorbable vascular scaffold deployment during percutaneous coronary intervention. EuroIntervention. 2014; [Epub ahead of print].
45. Ha J, Kim BK, Kim JS, et al. Assessing neointimal coverage after DES implantation by 3D OCT. JACC Cardiovasc Imaging. 2012;5:852–3.
46. Ughi GJ, Van Dyck CJ, Adriaenssens T, et al. Automatic assessment of stent neointimal coverage by intravascular optical coherence tomography. Eur Heart J Cardiovasc Imaging. 2014;15:195–200.

47. Slager CJ, Wentzel JJ, Schuurbiers JCH, et al. True 3-Dimensional reconstruction of coronary arteries in patients by fusion of angiography and IVUS (ANGUS) and its quantitative validation. Circulation. 2000;102:511–6.
48. Wahle A, Lopez JJ, Olszewski ME, et al. Plaque development, vessel curvature, and wall shear stress in coronary arteries assessed by X-ray angiography and intravascular ultrasound. Med Image Anal. 2006;10:615–31.
49. Tu S, Holm NR, Koning G, et al. Fusion of 3D QCA and IVUS/OCT. Int J Cardiovasc Imaging. 2011;27:197–207.
50.•• Tu S, Xu L, Ligthart J, et al. In-vivo comparison of arterial lumen dimensions assessed by co-registered three-dimensional (3D) quantitative coronary angiography, intravascular ultrasound and optical coherence tomography. Int J Cardiovasc Imaging. 2012;28:1315–27. *This papers describes the methodology for on-line co-registration of 3D-IVOCT with X-ray angiography, allowing for accurate and fast volumetric quantitative analysis of coronary artery lesions and stented segments*.
51. Hebsgaard L, Nielsen TM, Tu S, et al. Co-registration of optical coherence tomography and x-ray angiography in percutaneous coronary intervention. The Does Optical Coherence Tomography Optimize Revascularization (DOCTOR) Fusion study. J Am Coll Cardiol. 2013;62(18) Suppl 1:B203.
52.• Wang T, Wieser W, Springeling G, et al. Intravascular optical coherence tomography imaging at 3200 frames per second. Opt Lett. 2013;38:1715–7. *In this publication, a next-generation IVOCT catheter is described, enabling the acquisition of IVOCT pullbacks at very high frame-rate. Advancements in hardware like this, will further improve the image quality of 3D rendering.*
53. Ha J, Yoo H, Tearney GJ, Bouma BE. Compensation of motion artifacts in intracoronary optical frequency domain imaging and optical coherence tomography. Int J Cardiovasc Imaging. 2012;28:1299–304.